Predicting spacecraft surface degradation under atomic oxygen in Low Earth Orbit: supplemental document

CONTENTS

1. DEFINITIONS OF THE COORDINATE SYSTEMS

An outline of the coordinate systems and associated angular parameters employed in the erosion model is presented here, with their definitions illustrated in Fig. S1. The figure depicts two reference frames: a global frame and a local frame. In the global frame, the $\mathbf{z_G}$ axis is defined as the normal to the mean surface plane, while the $\mathbf{x_G}$ axis corresponds to the projection of the mean gas-flow direction onto that plane, i.e.

$$\mathbf{x_G} = \frac{\bar{\mathbf{v}}_\mathbf{i} - (\bar{\mathbf{v}}_\mathbf{i} \cdot \mathbf{z_G})\,\mathbf{z_G}}{\|\bar{\mathbf{v}}_\mathbf{i} - (\bar{\mathbf{v}}_\mathbf{i} \cdot \mathbf{z_G})\,\mathbf{z_G}\|}, \quad \text{where} \quad \bar{\mathbf{v}}_\mathbf{i} = \frac{\int_{\mathbf{v_i}\cdot\mathbf{z_G}<0} p(\mathbf{v_i})\mathbf{v_i}\ \mathrm{d}\,\mathbf{v_i}}{\int_{\mathbf{v_i}\cdot\mathbf{z_G}<0} p(\mathbf{v_i})\ \mathrm{d}\,\mathbf{v_i}}. \tag{1.1}$$

In this expression, $\mathbf{v}_i$ denotes the instantaneous incident gas-velocity vector, given by the sum of the mean incident velocity $\bar{\mathbf{v}}_i$ and a Gaussian-distributed random thermal component determined by the gas temperature. It is defined as

$$\mathbf{v_i}|^G = \begin{bmatrix} \sin(\theta_{i_1})\cos(\theta_{i_2}) \\ \sin(\theta_{i_1})\sin(\theta_{i_2}) \\ -\cos(\theta_{i_1}) \end{bmatrix} v_i, \tag{1.2}$$

with $\theta_{i_1} \in [0, \pi)$ and $\theta_{i_2} \in [0, 2\pi)$ being the global incidence angles, and $p(\mathbf{v_i})$ is its associated probability density function (PDF). When the incident velocity vector $\bar{\mathbf{v}}_\mathbf{i}$ is parallel to $\mathbf{z_G}$, we define $\mathbf{x_G}$ via any random vector that is perpendicular to $\mathbf{z_G}$. The global $\mathbf{y_G}$ axis is retrieved as $\mathbf{y_G} = \mathbf{z_G} \times \mathbf{x_G}$. The local reference frame, defined by axes $\mathbf{x_L}$, $\mathbf{y_L}$ and $\mathbf{z_L}$, has the former axis in the direction of the local surface normal vector $\mathbf{n_L}|^G = \begin{bmatrix} \sin(\theta_{n_1})\cos(\theta_{n_2}) & \sin(\theta_{n_1})\sin(\theta_{n_2}) & \cos(\theta_{n_1}) \end{bmatrix}^T$, where $\theta_{n_1} \in \left[0, \frac{\pi}{2}\right)$ and $\theta_{n_2} \in [0, 2\pi)$ are the normal angles. The $\mathbf{x_L}$ axis is then given as

$$\mathbf{x_L} = \frac{\mathbf{n_L} - (\mathbf{n_L} \cdot \mathbf{z_G})\,\mathbf{z_G}}{\|\mathbf{n_L} - (\mathbf{n_L} \cdot \mathbf{z_G})\,\mathbf{z_G}\|}, \tag{1.3}$$

and $\theta_{i_1} \in [0,\pi)$, $\theta_{i_2} \in [0,2\pi)$ are the instantaneous incidence angles. We default to $\mathbf{x_L} = \mathbf{x_G}$ when $\mathbf{n_L} \times \mathbf{z_G} = 0$. Likewise, the $\mathbf{y_L}$ axis is computed as $\mathbf{y_L} = \mathbf{z_L} \times \mathbf{x_L}$. The reflected velocity vector, $\mathbf{v_r}$, can be expressed in both the local and global reference frames via the reflected angle sets $(\theta_{r_1}, \theta_{r_2})$ and $(\theta_{l_1}, \theta_{l_2})$, with $\theta_{r_1} \in [0,\pi)$, $\theta_{r_2} \in [0,2\pi)$ and $\theta_{l_1} \in [0, \frac{\pi}{2})$, $\theta_{r_2} \in [0,2\pi)$. In the global frame, $\mathbf{v_r}$ takes the form $\mathbf{v_r}|^G = \begin{bmatrix}\sin(\theta_{r_1})\cos(\theta_{r_2}) & \sin(\theta_{r_1})\sin(\theta_{r_2}) & \cos(\theta_{r_1})\end{bmatrix}^T$, whereas in the local frame, it is written as $\mathbf{v_r}|^L = \begin{bmatrix}\sin(\theta_{l_1})\cos(\theta_{l_2}) & \sin(\theta_{l_1})\sin(\theta_{l_2}) & \cos(\theta_{l_1})\end{bmatrix}^T$. Changing the reference frame from the local to the global frame is achieved via elementary matrix rotations:

$$\mathbf{v_r}|^G = T_z(-\theta_{n_2})T_y(-\theta_{n_1})\ \mathbf{v_r}|^L,$$
$$\text{where} \quad T_z(\theta) = \begin{bmatrix}\cos(\theta) & \sin(\theta) & 0\\ -\sin(\theta) & \cos(\theta) & 0\\ 0 & 0 & 1\end{bmatrix}, \quad T_y(\theta) = \begin{bmatrix}\cos(\theta) & 0 & -\sin(\theta)\\ 0 & 1 & 0\\ \sin(\theta) & 0 & \cos(\theta)\end{bmatrix}. \tag{1.4}$$

From Eq. (1.4), a bijective transformation is defined, $(\theta_{r_1}, \theta_{r_2}) = \mathcal{T}(\theta_{l_1}, \theta_{l_2})$ and $(\theta_{l_1}, \theta_{l_2}) = \mathcal{T}^{-1}(\theta_{r_1}, \theta_{r_2})$. The first part of it is given as

$$\theta_{r_1}(\theta_{l_1}, \theta_{l_2}, \theta_{n_1}, \theta_{n_2}) = \arccos\left[\cos(\theta_{n_1})\cos(\theta_{l_1}) - \sin(\theta_{n_1})\sin(\theta_{l_1})\cos(\theta_{l_2})\right] \tag{1.5}$$

$$\theta_{r_2}(\theta_{l_1}, \theta_{l_2}, \theta_{n_1}, \theta_{n_2}) = \arctan\left[\frac{\sin(\theta_{n_2})C + \cos(\theta_{n_2}\sin(\theta_{l_1})\sin(\theta_{l_2})}{\cos(\theta_{n_2})C - \sin(\theta_{n_2})\sin(\theta_{l_1})\sin(\theta_{l_2})}\right], \tag{1.6}$$

$$\text{where} \quad C = \cos(\theta_{n_1})\sin(\theta_{l_1})\cos(\theta_{l_2}) + \sin(\theta_{n_1})\cos(\theta_{l_1}). \tag{1.7}$$

Consequently, the Jacobian matrix of this transformation, $J_L^R(\theta_{r_1}, \theta_{r_2}, \theta_{l_1}, \theta_{l_2})$, is easily derived to be

$$J_L^R(\theta_{r_1}, \theta_{r_2}, \theta_{l_1}, \theta_{l_2}) = \left|\frac{\partial(\theta_{r_1}, \theta_{r_2})}{\partial(\theta_{l_1}, \theta_{l_2})}\right| = \left|\frac{\sin(\theta_{l_1})}{\sin(\theta_{r_1})}\right|. \tag{1.8}$$

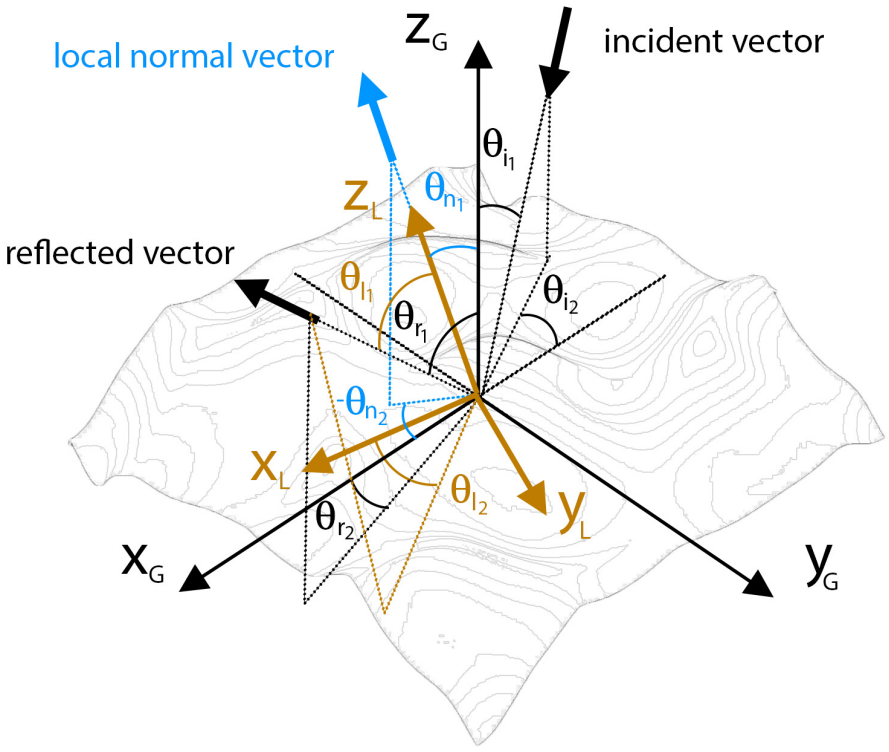

Fig. S1. Schematic of the coordinate frameworks used in the erosion model, with the associated angular definitions indicated. The signs of the angles correspond to a rotation from the global frame to the local frame.

2. STATISTICAL DEFINITION OF ROUGH SURFACES

A. Isotropic Surfaces: The poly-Gaussian Model

Statistical models of surface morphology have been extensively used in the literature [1, 2, 3], particularly within the context of electromagnetic wave scattering. Although not strictly required for spacecraft erosion modelling, such representations enable analytical treatment of complex multiple-scattering phenomena [4], or at minimum, facilitate dimensionality reduction. Among these, poly-Gaussian processes provide the most general and compact statistical description of geometrically rough surfaces. Originally introduced in [5] to model height distributions, they were later extended in [4] to incorporate slope statistics as well. Letting $\xi : \mathbb{R}^2 \to \mathbb{R}$, $\xi = \xi(x, y)$ be a function describing the height profile of a surface, the poly-Gaussian model defines it as

$$\xi(x, y) = \sigma(x, y)\epsilon(x, y) + \mu(x, y), \tag{2.1}$$

where $\mu, \sigma : \mathbb{R}^2 \to \mathbb{R}$ are C^∞ continuous stochastic functions defining the local mean and variance of the surface height ξ at point $\begin{bmatrix} x & y & \xi(x,y) \end{bmatrix}^T$. On the other hand, $\epsilon : \mathbb{R}^2 \to \mathbb{R}$ is a steady-state ergodic Gaussian process with zero mean and unit variance, i.e. $\epsilon \in \mathcal{G}(0, 1)$. To express μ and σ analytically, an additional control process $\gamma : \mathbb{R}^2 \to \mathbb{R}$ is introduced, defined as $\gamma = \gamma(x, y)$, which is assumed to be a stationary, ergodic Gaussian process with zero mean and unit variance i.e. $\gamma \sim \mathcal{G}(0, 1)$. Imposing isotropy allows a further reduction in dimensionality by transforming the Cartesian coordinates (x, y) into a radial variable $r = \sqrt{x^2 + y^2}$, leading to a surface profile of the form:

$$\xi(r) = \sigma\left(\gamma(r)\right)\epsilon\left(\gamma(r)\right) + \mu\left(\gamma(r)\right), \tag{2.2}$$

where $\mu : \mathbb{R} \to \mathbb{R}$ and $\sigma : \mathbb{R} \to \mathbb{R}$ are, this time, deterministic functions that represent non-linear transformations of the control process γ. When written in this form, it was shown that the probability density function (PDF) of the height profile $\xi(r)$ is [5]

$$p_h(\xi) = \int_{-\infty}^{\infty} p_\gamma(\gamma)\mathcal{G}\left(\xi, \mu(\gamma), \sigma(\gamma)\right)\, \mathrm{d}\,\gamma, \tag{2.3}$$

where $\mathcal{G}\left(\xi, \mu(\gamma), \sigma(\gamma)\right)$ is the Gaussian

$$\mathcal{G}\left(\xi, \mu(\gamma), \sigma(\gamma)\right) = \frac{1}{\sigma(\gamma)\sqrt{2\pi}} \exp\left[-\frac{\left(\xi - \mu(\gamma)\right)^2}{2\sigma(\gamma)^2}\right], \tag{2.4}$$

and the PDF of the γ process is just the normal distribution, i.e.

$$p_\gamma(\gamma) = \mathcal{G}\left(\gamma, 0, 1\right) = \frac{1}{\sqrt{2\pi}} \exp\left[-\frac{\gamma^2}{2}\right]. \tag{2.5}$$

Similarly, the PDF of the slope profile $\dot{\xi} = \frac{\mathrm{d}\,\xi}{\mathrm{d}\,r}$ was derived in [4] as

$$p_s(\dot{\xi}) = \int_{-\infty}^{\infty}\int_{-\infty}^{\infty} p_\gamma(\gamma)p_{\dot{\gamma}}(\dot{\gamma})\mathcal{G}\left(\dot{\xi}, \mu_s(\gamma, \dot{\gamma}), \sigma_s(\gamma, \dot{\gamma})\right)\, \mathrm{d}\,\gamma\, \mathrm{d}\,\dot{\gamma}, \tag{2.6}$$

where the Gaussian function $\mathcal{G}\left(\dot{\xi}, \mu_s(\gamma, \dot{\gamma}), \sigma_s(\gamma, \dot{\gamma})\right)$ is given as

$$\mathcal{G}\left(\dot{\xi}, \mu_s(\gamma, \dot{\gamma}), \sigma_s(\gamma, \dot{\gamma})\right) = \frac{1}{\sigma_s\sqrt{2\pi}} \exp\left[-\frac{\left(\dot{\xi} - \mu_s(\gamma, \dot{\gamma})\right)^2}{2\sigma_s(\gamma, \dot{\gamma})^2}\right], \tag{2.7}$$

and the PDF of the radial derivative of the γ process, $\dot{\gamma} = \frac{\mathrm{d}\,\gamma}{\mathrm{d}\,r}$ is given as in [4]:

$$p_{\dot{\gamma}}(\dot{\gamma}) = \mathcal{G}\left(\dot{\gamma}, 0, \frac{\sqrt{2}}{R}\right) = \frac{R}{\sqrt{4\pi}} \exp\left[-\frac{R^2\dot{\gamma}^2}{4}\right]. \tag{2.8}$$

The slope mean and variance functions, $\mu_s(\gamma, \dot{\gamma})$ and $\sigma_s(\gamma, \dot{\gamma})$, are defined as

$$\begin{aligned} \mu_s(\gamma, \dot{\gamma}) &= \frac{\mathrm{d}\,\mu(\gamma)}{\mathrm{d}\,\gamma}\dot{\gamma}, \\ \sigma_s(\gamma, \dot{\gamma}) &= \sqrt{2\left(\frac{\sigma(\gamma)}{R}\right)^2 + \dot{\gamma}^2\left(\frac{\mathrm{d}\,\sigma(\gamma)}{\mathrm{d}\,\gamma}\right)^2}. \end{aligned} \tag{2.9}$$

The ϵ and γ processes have autocorrelation functions $\mathcal{C}_\epsilon, \mathcal{C}_\gamma : [0,\infty) \to \mathbb{R}$ of the form

$$\mathcal{C}_i(r) = \exp\left[-\frac{r^2}{R^2}\right], \quad \text{with} \quad i = \{\epsilon, \gamma\}, \tag{2.10}$$

where R is the autocorrelation length. Another important quantity pertaining to the statistical description of surface morphology is the shadowing function $\mathcal{S} : [0,\pi] \times \mathbb{R} \times [0,\infty) \to [0,1]$, $\mathcal{S} = \mathcal{S}(\theta_{r_1}, \xi_0, r)$, defined in the global reference frame and describing the probability that a particle residing at height ξ_0 and travelling at angle θ, will travel a horizontal distance r from its origin without colliding with the surface. This shadow function has the expression [4]

$$\mathcal{S}(\theta_{r_1}, \xi_0, r) = \left(\frac{F_h(\xi_0)}{F_h(\xi_0 + \eta r)}\right)^{D(\theta_{r_1})}, \tag{2.11}$$

where the cumulative density function (CDF) $F(\xi)$ is given by

$$F_h(\xi) = \int_{-\infty}^{\infty} P(\gamma)\frac{1}{2}\left[1 + \operatorname{erf}\left(\frac{\xi - \mu(\gamma)}{\sigma(\gamma)\sqrt{2}}\right)\right] \mathrm{d}\,\gamma, \tag{2.12}$$

and the exponent, $D(\theta_{r_1})$ has the form

$$\begin{aligned} D(\theta_{r_1}) &= \int_{\infty}^{\infty}\int_{\infty}^{\infty} p_\gamma(\gamma)\, p_{\dot\gamma}(\dot\gamma)\, \Delta(\theta_{r_1} \,|\, \gamma, \dot\gamma)\ \mathrm{d}\,\gamma\, \mathrm{d}\,\dot\gamma \\ \text{with} \quad \Delta(\theta_{r_1} \,|\, \gamma, \dot\gamma) &= \frac{\sigma_s(\gamma,\dot\gamma)}{\sqrt{2\pi}} \exp\left[-\frac{(\eta - \mu_s(\gamma,\dot\gamma))^2}{2\sigma_s(\gamma,\dot\gamma)^2}\right] \\ &\quad - \frac{1}{2}\left(\eta - \mu_s(\gamma,\dot\gamma)\right) \operatorname{erfc}\left[\frac{\eta - \mu_s(\gamma,\dot\gamma)}{\sigma_s(\gamma,\dot\gamma)\sqrt{2}}\right], \end{aligned} \tag{2.13}$$

and the variable $\eta = 1/\tan(\theta_{r_1})$. If one takes the limit of $r \to \infty$ of the above expression, then one obtains the probability of a particle escaping the surface, given its initial height ξ_0 and reflection angle θ_{r_1},

$$\lim_{r\to\infty} \mathcal{S}(\theta_{r_1}, \xi_0, r) = \mathcal{S}(\theta_{r_1}, \xi_0) = F_h(\xi_0)^{D(\theta_{r_1})}. \tag{2.14}$$

B. Anisotropic "Angled" Surfaces: The Biased poly-Gaussian Model

Although ram-facing spacecraft surfaces typically erode in an isotropic manner [6], this behaviour does not extend to other orientations. Panels inclined to the flow are etched along the incoming direction, developing anisotropic morphologies characterised by concave cavities that cannot be represented by a single-valued height function [7]. To solve this, the coordinate system in which the poly-Gaussian model is defined is rotated by the mean incidence angle of the incoming AO atoms in the +y axis (denoted henceforth as θ_s), as shown in Fig. S2. Then, the height profile of the surface, $\xi : \mathbb{R}^2 \to \mathbb{R}$, $\xi = \xi(x,y)$, is written as

$$\xi(x,y) = \hat\xi(x) + \xi'(x,y), \tag{2.15}$$

where $\hat\xi(x) = -\tan(\theta_s)x$ is a deterministic bias that depends only on x, and $\xi'(x,y)$ is an isotropic poly-Gaussian process defined by Eq. (2.2). Written in spherical coordinates, defined by the radial variable r and global angles θ_{r_1} and θ_{r_2}, the surface profile becomes

$$\xi(r, \theta_{r_2}) = -\tan(\theta_s)\cos(\theta_{r_2})r + \xi'(r). \tag{2.16}$$

The corresponding height PDF then depends on r and θ_{r_2} and takes the form

$$P(\xi, |r, \theta_{r_2}) = \int_{-\infty}^{\infty} P(\xi')P(\xi - \xi')\ \mathrm{d}\,\xi'. \tag{2.17}$$

Remembering that $P(\xi')$ is given by Eq. (2.3), and that the quantity $\xi - \xi'$ is deterministic with an expression given by Eq. (2.16), the height PDF can be written as

$$P(\xi \,|\, r, \theta_{r_2}) = \int_{-\infty}^{\infty} p_h(\xi')\delta(\xi - \xi' + \tan(\theta_s)\cos(\theta_{r_2})r)\ \mathrm{d}\,\xi' \tag{2.18}$$

$$= p_h\left(\xi + \tan(\theta_s)\cos(\theta_{r_2})r\right), \tag{2.19}$$

which shows that it retains the form of the poly-Gaussian height PDF, shifted by the term $\tan(\theta_s)\cos(\theta_{r_2})r$. Expanding this PDF, we obtain

$$\begin{aligned} p_h(\xi + \tan(\theta_s)\cos(\theta_{r_2})r) &= \int_{-\infty}^{\infty} p_\gamma(\gamma)\mathcal{G}\left(\xi + \tan(\theta_s)\cos(\theta_{r_2})r, \mu(\gamma), \sigma(\gamma)\right)\,\mathrm{d}\,\gamma \\ &= \int_{-\infty}^{\infty} p_\gamma(\gamma)\mathcal{G}\left(\xi, \mu(\gamma) - \tan(\theta_s)\cos(\theta_{r_2})r, \sigma(\gamma)\right)\,\mathrm{d}\,\gamma \\ &= \int_{-\infty}^{\infty} p_\gamma(\gamma)\mathcal{G}\left(\xi, \mu^b(\gamma, r, \theta_{r_2}), \sigma(\gamma)\right)\,\mathrm{d}\,\gamma \\ &= p_h^b(\xi). \end{aligned} \tag{2.20}$$

Thus, the height PDF of the angled surface profile is still expressed within the poly-Gaussian framework, with the deterministic bias acting as a correction to the mean process, $\mu^b(\gamma, r, \theta_{r_2}) = \mu(\gamma) - \tan(\theta_s)\cos(\theta_{r_2})r$.

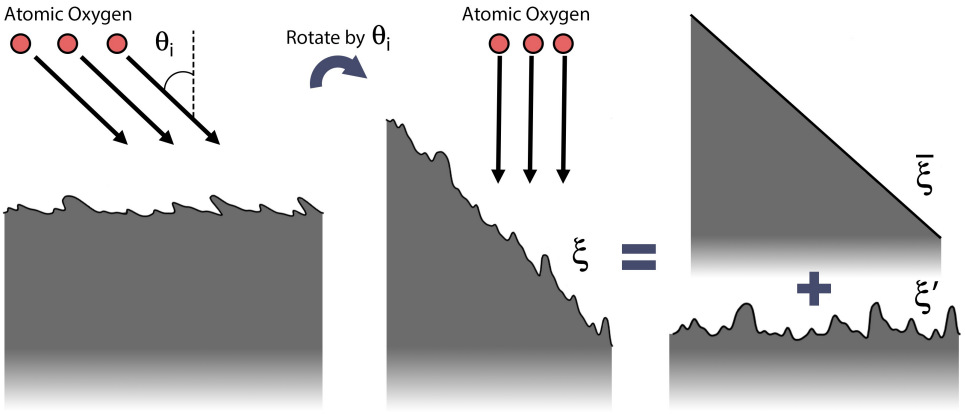

Fig. S2. Illustration of "angled" anisotropic roughness. After rotating the frame by angle θ_i, the surface decomposes into a constant slope component $\hat{\xi}$ and an isotropic poly-Gaussian roughness ξ'.

The slope profile of the angled surface defined in Eq. (2.16) is defined as

$$\dot{\xi}(r, \theta_{r_2}) = \frac{\partial \xi(r, \theta_{r_2})}{\partial r} = -\tan(\theta_s)\cos(\theta_{r_2}) + \dot{\xi}'(r), \tag{2.21}$$

taking the same form as the unbiased poly-Gaussian slope process $\dot{\xi}'(r)$, biased by the constant term $-\tan(\theta_s)\cos(\theta_{r_2})$. Therefore, deriving its slope PDF, $p_s^b(\dot{\xi})$ follows the same procedure as the height PDF derivation, leading to

$$\begin{aligned} p_s^b(\dot{\xi}) &= P\left(\dot{\xi} + \tan(\theta_s)\cos(\theta_{r_2})\right) \\ &= \int_{-\infty}^{\infty}\int_{-\infty}^{\infty} p_\gamma(\gamma)p_{\dot{\gamma}}(\dot{\gamma})\mathcal{G}\left(\dot{\xi} + \tan(\theta_s)\cos(\theta_{r_2}), \mu_s(\gamma, \dot{\gamma}), \sigma_s(\gamma, \dot{\gamma})\right)\,\mathrm{d}\,\dot{\gamma}\,\mathrm{d}\,\gamma \\ &= \int_{-\infty}^{\infty}\int_{-\infty}^{\infty} p_\gamma(\gamma)p_{\dot{\gamma}}(\dot{\gamma})\mathcal{G}\left(\dot{\xi}, \mu_s(\gamma, \dot{\gamma}) - \tan(\theta_s)\cos(\theta_{r_2}), \sigma_s(\gamma, \dot{\gamma})\right)\,\mathrm{d}\,\dot{\gamma}\,\mathrm{d}\,\gamma \\ &= \int_{-\infty}^{\infty}\int_{-\infty}^{\infty} p_\gamma(\gamma)p_{\dot{\gamma}}(\dot{\gamma})\mathcal{G}\left(\dot{\xi}, \mu_s^b(\gamma, \dot{\gamma}, \theta_{r_2}), \sigma_s(\gamma, \dot{\gamma})\right)\,\mathrm{d}\,\dot{\gamma}\,\mathrm{d}\,\gamma. \end{aligned} \tag{2.22}$$

The above expression is also expressed within the poly-Gaussian framework, much like that in Eq. (2.20), with the mean slope process being corrected by the deterministic constant bias $\mu_s^b(\gamma, \dot{\gamma}, \theta_{r_2}) = \mu_s(\gamma, \dot{\gamma}) - \tan(\theta_s)\cos(\theta_{r_2})$. The final quantity to be derived for the biased poly-Gaussian model is the shadowing function $\mathcal{S}^b : [0, \pi] \times [0, 2\pi] \times \mathbb{R} \times [0, \infty) \to [0, 1]$, $\mathcal{S}^b = \mathcal{S}^b(\theta_{r_1}, \theta_{r_2}, \xi_0, r)$, defined in the global reference frame and having the same meaning as for the unbiased poly-Gaussian model. Starting from Eq. (9) from [8], this function is written as

$$\mathcal{S}^b(\theta_{r_1}, \theta_{r_2}, \xi_0, r) = \mathcal{S}^b(\theta_{r_1}, \theta_{r_2}, \xi_0, 0)\exp\left[-\int_0^r g(\tau)\,\mathrm{d}\,\tau\right], \tag{2.23}$$

where $g(\tau)\Delta\tau$ is the probability that a gas particle hits the surface in $(\tau, \tau+\Delta\tau)$, given that it has not until τ. In the equation above, $\mathcal{S}^b(\theta_{r_1}, \theta_{r_2}, \xi_0, 0) = 1$, by definition. Then, the shadowing function becomes

$$\mathcal{S}^b(\theta_{r_1}, \theta_{r_2}, \xi_0, r) = \exp\left[-\Gamma(\theta_{r_1}, \theta_{r_2}) \int_0^r \frac{p_h^b(\xi_0 + \eta\tau)}{F_h^b(\xi_0 + \eta\tau)} \, \mathrm{d}\,\tau\right], \tag{2.24}$$

where $\eta = \frac{1}{\tan(\theta_{r_1})}$ and

$$\Gamma(\theta_{r_1}, \theta_{r_2}) = \int_\eta^\infty (\dot{\xi} - \eta)\, p_s^b\,(\dot{\xi}) \, \mathrm{d}\,\dot{\xi}. \tag{2.25}$$

One can see that both expressions contain the previously derived height and slope PDFs for angled surfaces, which is consistent with the biased poly-Gaussian formalism. From a numerical standpoint, however, it is far more convenient to express $\mathcal{S}^b(\theta_{r_1}, \theta_{r_2}, \xi_0, r)$ directly in terms of the bounded $\mu(\gamma)$, $\sigma(\gamma)$, $\mu_s(\gamma, \dot{\gamma})$ and $\sigma_s(\gamma, \dot{\gamma})$ processes of the unbiased poly-Gaussian model. Hence,

$$\begin{aligned}\mathcal{S}^b(\theta_{r_1}, \theta_{r_2}, \xi_0, r) &= \exp\left[-\Gamma(\theta_{r_1}, \theta_{r_2}) \int_0^r \frac{p_h\left(\xi_0' + \eta\tau + \tan(\theta_s)\cos(\theta_{r_2})\tau\right)}{F_h(\xi_0' + \eta\tau + \tan(\theta_s)\cos(\theta_{r_2})\tau)} \, \mathrm{d}\,\tau\right] \\ &= \exp\left[-\Gamma(\theta_{r_1}, \theta_{r_2}) \int_0^r \frac{p_h(\xi_0' + \eta^b\tau)}{F_h(\xi_0' + \eta^b\tau)} \, \mathrm{d}\,\tau\right].\end{aligned} \tag{2.26}$$

where $\eta^b = \eta + \tan(\theta_s)\cos(\theta_{r_2})$, and it was assumed that $\xi_0 = \xi_0'$ at $r = 0$. Likewise,

$$\begin{aligned}\Gamma(\theta_{r_1}, \theta_{r_2}) &= \int_\eta^\infty (\dot{\xi} - \eta)\, p_s\,(\dot{\xi} + \tan(\theta_s)\cos(\theta_{r_2})) \, \mathrm{d}\,\dot{\xi} \\ &= \int_{\eta + \tan(\theta_s)\cos(\theta_{r_2})}^\infty (\dot{\xi}' - \tan(\theta_s)\cos(\theta_{r_2}) - \eta)\, p_s\,(\dot{\xi}') \, \mathrm{d}\,\dot{\xi}' \\ &= \int_{\eta^b}^\infty \left(\dot{\xi}' - \eta^b\right) p_s\,(\dot{\xi}') \, \mathrm{d}\,\dot{\xi}'.\end{aligned} \tag{2.27}$$

Since both expressions coincide with those of the shadowing function for the unbiased poly-Gaussian model outlined in [4], with η being substituted for η^b, the rest of the derivation will proceed in a very similar manner. Changing variables from τ to $h = \xi_0' + \eta^b\tau$ leads to

$$\begin{aligned}\mathcal{S}^b(\theta_{r_1}, \theta_{r_2}, \xi_0, r) &= \exp\left[-\frac{\Gamma(\theta_{r_1}, \theta_{r_2})}{\eta^b} \int_{\xi_0'}^{\xi'} \frac{p_h\,(h)}{F_h(h)} \, \mathrm{d}\,h\right] \\ &= \exp\left[-\frac{\Gamma(\theta_{r_1}, \theta_{r_2})}{\eta^b} \int_{F_h(\xi_0')}^{F_h(\xi')} \frac{1}{F_h(h)} \, \mathrm{d}\,F_h(h)\right] \\ &= \exp\left[-D^b(\theta_{r_1}, \theta_{r_2}) \ln\left(\frac{F_h(\xi')}{F_h(\xi_0')}\right)\right] \\ &= \left(\frac{F_h(\xi_0')}{F_h(\xi')}\right)^{D^b(\theta_{r_1}, \theta_{r_2})}.\end{aligned} \tag{2.28}$$

where $\xi' = \xi_0' + \eta^b r$ and the exponent $D^b(\theta_{r_1}, \theta_{r_2})$ takes the form

$$\begin{aligned}D^b(\theta_{r_1}, \theta_{r_2}) &= \int_\infty^\infty \int_\infty^\infty p_\gamma(\gamma)\, p_{\dot{\gamma}}(\dot{\gamma})\, \Delta^b(\theta_{r_1}, \theta_{r_2} \,|\, \gamma, \dot{\gamma}) \, \mathrm{d}\,\gamma \, \mathrm{d}\,\dot{\gamma} \\ \text{with} \quad \Delta^b(\theta_{r_1}, \theta_{r_2} \,|\, \gamma, \dot{\gamma}) &= \frac{\sigma_s(\gamma, \dot{\gamma})}{\sqrt{2\pi}} \exp\left[-\frac{(\eta^b - \mu_s(\gamma, \dot{\gamma}))^2}{2\sigma_s(\gamma, \dot{\gamma})^2}\right] \\ &\quad - \frac{1}{2}\left(\eta^b - \mu_s(\gamma, \dot{\gamma})\right) \operatorname{erfc}\left[\frac{\eta^b - \mu_s(\gamma, \dot{\gamma})}{\sigma_s(\gamma, \dot{\gamma})\sqrt{2}}\right].\end{aligned} \tag{2.29}$$

This completes the derivation of the biased poly-Gaussian model for random rough surfaces, which has introduced the quantities $p_h^b(\xi)$, $F_h^b(\xi)$, $p_s^b(\dot{\xi})$, $F_s^b(\dot{\xi})$ and $\mathcal{S}^b(\theta_{r_1}, \theta_{r_2}, \xi_0, r)$. When the surface angle is set to $\theta_s = 0^\circ$, these expressions reduce to their unbiased poly-Gaussian counterparts, namely $p_h(\xi)$, $F_h(\xi)$, $p_s(\dot{\xi})$, $F_s(\dot{\xi})$ and $\mathcal{S}(\theta_{r_1}, \xi_0, r)$, which shows that the biased model is a generalisation of the unbiased one. In the following sections, we therefore work with the biased formulation to derive expressions for the scattering of atomic oxygen (AO) particles in different local regimes and to construct the associated erosion model.

3. DERIVATION OF ATOMIC OXYGEN SCATTERING LAWS

In this section, we apply the biased poly-Gaussian model to obtain analytical expressions for the scattering distribution of AO atoms from a random rough surface, considering several distinct local scattering regimes. We begin with the general form of this PDF,

$$\begin{aligned} p_{sct}\left(v_r, \theta_{r_1}, \theta_{r_2}\right) &= P\left(v_r, \theta_{r_1}, \theta_{r_2} \,|\, \mathbf{v_i}, \text{ surf. param., local param.}\right) \\ &= \mathcal{K}_K\left(\mathbf{v_i} \to \mathbf{v_r}\right) \left| \frac{\partial(v_{r_x}, v_{r_y}, v_{r_z})}{\partial\left(v_r, \theta_{r_1}, \theta_{r_2}\right)} \right| \\ &= \frac{1}{N(\mathbf{v_i})} \int_{\mathbf{v_i}\cdot\mathbf{n_L}<0} \mathcal{K}_L\left(\mathbf{v_{i_L}} \to \mathbf{v_{r_L}}\right) p_n(\mathbf{n_L}) \left|\mathbf{n_L}\cdot\mathbf{v_i}\right| \,\mathrm{d}\,\mathbf{n_L} \cdot v_r^2 \sin(\theta_{r_1}). \end{aligned} \tag{3.1}$$

where $\mathcal{K}_K\left(\mathbf{v_i} \to \mathbf{v_r}\right)$ is the single-reflection Kirchhoff kernel outlined in Eq. (109) of [4], $\mathcal{K}_L\left(\mathbf{v_{i_L}} \to \mathbf{v_{r_L}}\right)$ is the local scattering kernel, defining how gas particles would interact with the surface assuming no geometric roughness, and $\mathbf{n_L}$ and $p_n(\mathbf{n_L})$ are the local surface normal vector and its corresponding PDF. The normalisation factor $N(\mathbf{v_i})$ is defined as

$$\begin{aligned} N(\mathbf{v_i}) &= \int_{\mathbf{v_i}\cdot\mathbf{n_L}<0} p_n(\mathbf{n_L}) \left|\mathbf{n_L}\cdot\mathbf{v_i}\right| \,\mathrm{d}\,\mathbf{n_L} \\ &= \left| \left(\int_{\mathbf{v_i}\cdot\mathbf{n_L}<0} p_n(\mathbf{n_L}) \mathbf{n_L} \,\mathrm{d}\,\mathbf{n_L} \right) \cdot \mathbf{v_i} \right| \\ &= \left|\mathbf{n_G}\cdot\mathbf{v_i}\right|. \end{aligned} \tag{3.2}$$

where $\mathbf{n_G} = \begin{bmatrix}\sin(\theta_s) & 0 & \cos(\theta_s)\end{bmatrix}^T$ when the entire surface is in view, i.e. no shadowing occurs. The reader should note that the original expression for $\mathcal{K}_K\left(\mathbf{v_i} \to \mathbf{v_r}\right)$ in [4] contains a typographical error, and that Eq. (3.1) provides the corrected form used in this work. As discussed in the same study, Eq. (3.1) is too complex to write in a closed-form analytic expression, making it impractical to implement in an erosion model. Great simplicity can be achieved, however, if we rewrite the scattering PDF as

$$\begin{aligned} p_{sct}\left(v_r, \theta_{r_1}, \theta_{r_2}\right) &= p_{sct}^{vel}\left(v_r\right) \cdot p_{sct}^{ang}\left(\theta_{r_1}, \theta_{r_2}\right) \\ &= P\left(v_r \,|\, v_i, \text{ local vel. param}\right) \\ &\quad \cdot P\left(\theta_{r_1}, \theta_{r_2} \,|\, \theta_{i_1}, \theta_{i_2}, \text{ surf. param, local ang. param.}\right), \end{aligned} \tag{3.3}$$

where we are de-coupling the statistics of the reflected particle directions and velocity magnitudes. Assuming that the local kernel can also be decoupled into an angular kernel and a velocity magnitude kernel, i.e.

$$\mathcal{K}_L\left(\mathbf{v_{i_L}} \to \mathbf{v_{r_L}}\right) = \mathcal{K}_L^{vel}\left(v_{i_L} \to v_{r_L}\right) \mathcal{K}_L^{ang}\left(\theta_{i_{1_L}}, \theta_{i_{2_L}} \to \theta_{l_1}, \theta_{l_2}\right), \tag{3.4}$$

we transform Eq. (3.1) into a product of two such PDFs. The angular PDF is first written as an integral over the local surface normal:

$$p_{sct}^{ang}(\theta_{r_1}, \theta_{r_2}) = \int_{\mathbf{v_i}\cdot\mathbf{n_L}<0} \mathcal{K}_L^{ang}\left(\theta_{i_{1_L}}, \theta_{i_{2_L}} \to \theta_{l_1}, \theta_{l_2}\right) p_n(\mathbf{n_L}) \frac{\left|\mathbf{n_L}\cdot\mathbf{v_i}\right|}{\left|\mathbf{n_G}\cdot\mathbf{v_i}\right|} \,\mathrm{d}\,\mathbf{n_L} \cdot \sin(\theta_{r_1}). \tag{3.5}$$

Next, we factor out the speed by introducing the incident direction vector $\mathbf{u_i} = \mathbf{v_i}/v_i$:

$$p_{sct}^{ang}(\theta_{r_1}, \theta_{r_2}) = \int_{\mathbf{v_i}\cdot\mathbf{n_L}<0} \mathcal{K}_L^{ang}\left(\theta_{i_{1_L}}, \theta_{i_{2_L}} \to \theta_{l_1}, \theta_{l_2}\right) p_n(\mathbf{n_L}) \frac{\left|\mathbf{n_L}\cdot\mathbf{u_i}\right|}{\left|\mathbf{n_G}\cdot\mathbf{u_i}\right|} \,\mathrm{d}\,\mathbf{n_L} \cdot \sin(\theta_{r_1}). \tag{3.6}$$

We then rewrite the normal PDF p_n in terms of PDF over the surface slopes $(\dot{\xi}_x, \dot{\xi}_y)$, using the Jacobian of the mapping:

$$\begin{aligned} p_{sct}^{ang}(\theta_{r_1}, \theta_{r_2}) = \frac{\sin(\theta_{r_1})}{\left|\mathbf{n_G}\cdot\mathbf{u_i}\right|} \int_{\mathbf{v_i}\cdot\mathbf{n_L}<0} &\mathcal{K}_L^{ang}\left(\theta_{i_{1_L}}, \theta_{i_{2_L}} \to \theta_{l_1}, \theta_{l_2}\right) \\ &\cdot P(\dot{\xi}_x, \dot{\xi}_y \,|\, \sigma(\gamma), \mu(\gamma), R, \theta_{i_1}, \theta_{i_2}) \left(1 + \dot{\xi}_x^2 + \dot{\xi}_y^2\right)^{\frac{3}{2}} \\ &\cdot \left|\dot{\xi}_x \sin(\theta_{i_1}) \cos(\theta_{i_2}) + \dot{\xi}_y \sin(\theta_{i_1}) \sin(\theta_{i_2}) + \cos(\theta_{i_1})\right| \,\mathrm{d}\,\mathbf{n_L}. \end{aligned} \tag{3.7}$$

Finally, we rewrite the integral in terms of the polar angles of the local normal, $(\theta_{n_1}, \theta_{n_2})$, which yields:

$$\begin{aligned} p_{sct}^{ang}(\theta_{r_1}, \theta_{r_2}) = \frac{\sin(\theta_{r_1})}{|\mathbf{n_G} \cdot \mathbf{u_i}|} \int_0^{\frac{\pi}{2}} \int_0^{2\pi} \mathcal{K}_L^{ang}\left(\theta_{i_{1_L}}, \theta_{i_{2_L}} \to \theta_{l_1}, \theta_{l_2}\right) \mathcal{M}(\theta_{i_1}, \theta_{i_2}, \theta_{n_1}, \theta_{n_2}) \\ \cdot p_{s_{2D}}^b\left(-\tan(\theta_{n_1})\cos(\theta_{n_2}), -\tan(\theta_{n_1})\sin(\theta_{n_2})\right)\left(1+\tan^2(\theta_{n_1})\right)^{\frac{3}{2}} \\ \cdot \left|\cos(\theta_{i_1}) - \tan(\theta_{n_1})\sin(\theta_{i_1})\left(\cos(\theta_{n_2})\cos(\theta_{i_2}) + \sin(\theta_{n_2})\sin(\theta_{i_2})\right)\right| \\ \cdot \sin(\theta_{n_1})\, \mathrm{d}\,\theta_{n_2}\, \mathrm{d}\,\theta_{n_1} \end{aligned} \tag{3.8}$$

where $\mathcal{M}(\theta_{i_1}, \theta_{i_2}, \theta_{n_1}, \theta_{n_2})$ is a masking function, enforcing the condition $\mathbf{v_i} \cdot \mathbf{n_L} < 0$. The 2D surface slope PDF, $p_{s_{2D}}^b\left(\dot{\xi}_x, \dot{\xi}_y\right)$, is given by

$$\begin{aligned} p_{s_{2D}}^b\left(\dot{\xi}_x, \dot{\xi}_y\right) = \int_{-\infty}^{\infty}\int_{-\infty}^{\infty}\int_{-\infty}^{\infty} p_\gamma(\gamma) p_{\dot{\gamma}}(\dot{\gamma}_x) p_{\dot{\gamma}}(\dot{\gamma}_y) \mathcal{G}\left(\dot{\xi}_x, \mu_s^b(\gamma, \dot{\gamma}_x, \theta_{r_2}), \sigma_s(\gamma, \dot{\gamma}_x)\right) \\ \cdot \mathcal{G}\left(\dot{\xi}_y, \mu_s(\gamma, \dot{\gamma}_y, \theta_{r_2}), \sigma_s(\gamma, \dot{\gamma}_y)\right)\, \mathrm{d}\,\dot{\gamma}_x\, \mathrm{d}\,\dot{\gamma}_y\, \mathrm{d}\,\gamma. \end{aligned} \tag{3.9}$$

We now shift our attention to the velocity magnitude PDF,

$$p_{sct}^{vel}(v_r) = v_r^2 \mathcal{K}_L^{vel}(v_{i_L} \to v_{r_L}). \tag{3.10}$$

Since the global to local coordinate transformation does not affect velocity magnitudes, we can rewrite this expression in the global reference frame as

$$p_{sct}^{vel}(v_r) = v_r^2 \mathcal{K}_L^{vel}(v_i \to v_r). \tag{3.11}$$

Eqs. (3.8) and (3.11) represent the final expressions for the angular and velocity components of the scattering kernel $p_{sct}\left(v_r, \theta_{r_1}, \theta_{r_2}\right)$ written in their most general form. To further define them, we now need to choose suitable local kernels $\mathcal{K}_L^{ang}\left(\theta_{i_{1_L}}, \theta_{i_{2_L}} \to \theta_{l_1}, \theta_{l_2}\right)$ and $\mathcal{K}_L^{vel}\left(v_{i_L} \to v_{r_L}\right)$. For the velocity kernel $\mathcal{K}_L^{vel}\left(v_i \to v_r\right)$, we select an incomplete accommodation model of the form

$$\begin{aligned} \mathcal{K}_L^{vel}\left(v_{i_L} \to v_{r_L}\right) = \frac{1}{2}\left(\frac{\mu_{AO}}{RT}\right)^4 v_{r_L} \exp\left[-\frac{\mu_{AO} v_{r_L}^2}{2RT}\right] \\ \text{with} \quad T = (1-\alpha_E)\, T_i + \alpha_E\, T_S, \quad \text{and} \quad T_i = \frac{\mu_{AO} v_{i_L}^2}{3R}. \end{aligned} \tag{3.12}$$

In the expression above, R denotes the ideal gas constant, μ_{AO} is the molar mass of AO, and α_E and T_S are the surface energy accommodation coefficient and surface temperature. The rationale for this particular choice of velocity kernel is discussed in the main body of this work. The angular scattering kernel $\mathcal{K}_L^{ang}\left(\theta_{i_{1_L}}, \theta_{i_{2_L}} \to \theta_{l_1}, \theta_{l_2}\right)$, however, requires a more careful treatment. In [4] it was shown that gas particles scattering from rough surfaces exhibit a mixture of quasi specular and diffuse reflections that depends on the incidence angle. Since satellite surfaces subjected to AO erosion are strongly roughened, a similar behaviour is expected here. A convenient way to represent this is to adopt a Maxwell type model, that is, a linear combination of a purely diffuse and a purely specular local kernel. The fraction of gas particles that scatter diffusely is taken to be equal to the energy accommodation coefficient α_E. The final local angular kernel expression is then given as

$$\mathcal{K}_L^{ang}\left(\theta_{i_1}, \theta_{i_2} \to \theta_{r_1}, \theta_{r_2}\right) = (1-\alpha_E)\, \mathcal{K}_{L_{spec}}^{ang}\left(\theta_{i_1}, \theta_{i_2} \to \theta_{r_1}, \theta_{r_2}\right) + \alpha_E\, \mathcal{K}_{L_{diff}}^{ang}\left(\theta_{i_1}, \theta_{i_2} \to \theta_{r_1}, \theta_{r_2}\right). \tag{3.13}$$

Similarly, via the linearity of the problem, the final angular scattering PDF will have the form

$$p_{sct}^{ang}(\theta_{r_1}, \theta_{r_2}) = (1-\alpha_E)\, p_{spec}^{ang}(\theta_{r_1}, \theta_{r_2}) + \alpha_E\, p_{diff}^{ang}(\theta_{r_1}, \theta_{r_2}). \tag{3.14}$$

In the following subsections we derive the corresponding expressions for both $p_{spec}^{ang}(\theta_{r_1}, \theta_{r_2})$ and $p_{diff}^{ang}(\theta_{r_1}, \theta_{r_2})$.

A. Scattering Under Locally-Diffuse Reflections

The expression of a local angular reflection kernel under the assumption of fully-diffuse reflections is given by the cosine law:

$$\begin{aligned}\mathcal{K}^{ang}_{L_{diff}}\left(\theta_{i_{1_L}},\theta_{i_{2_L}}\rightarrow\theta_{l_1},\theta_{l_2}\right) &= \frac{\left|\cos(\theta_{l_1})\right|}{\pi}\\ &= \frac{1}{\pi}\left|\sin(\theta_{r_1})\sin(\theta_{n_1})\cos(\theta_{r_2}-\theta_{n_2})+\cos(\theta_{r_1})\cos(\theta_{n_1})\right|,\end{aligned} \tag{3.15}$$

and thus is independent of the incidence angles θ_{i_1} and θ_{i_2}. Furthermore, the condition $\cos(\theta_{l_1}) \leq 0$ coincides with the condition $\mathbf{v_i}\cdot\mathbf{n_L}\geq 0$. As such, we can eliminate the need for a masking function $\mathcal{M}(\theta_{i_1},\theta_{i_2},\theta_{n_1},\theta_{n_2})$ in Eq. (3.8), leading to the diffuse scattering PDF taking the form

$$\begin{aligned}p^{ang}_{diff}(\theta_{r_1},\theta_{r_2}) = \frac{\sin(\theta_{r_1})}{|\mathbf{n_G}\cdot\mathbf{u_i}|}\int_0^{\frac{\pi}{2}}\int_0^{2\pi} Max\left(0,\frac{1}{\pi}\left|\sin(\theta_{r_1})\sin(\theta_{n_1})\cos(\theta_{r_2}-\theta_{n_2})+\cos(\theta_{r_1})\cos(\theta_{n_1})\right|\right)\\ \cdot p^b_{s_{2D}}\left(-\tan(\theta_{n_1})\cos(\theta_{n_2}),-\tan(\theta_{n_1})\sin(\theta_{n_2})\right)\left(1+\tan^2(\theta_{n_1})\right)^{\frac{3}{2}}\\ \cdot\left|\cos(\theta_{i_1})-\tan(\theta_{n_1})\sin(\theta_{i_1})\left(\cos(\theta_{n_2})\cos(\theta_{i_2})+\sin(\theta_{n_2})\sin(\theta_{i_2})\right)\right|\\ \cdot\sin(\theta_{n_1})\ \mathrm{d}\,\theta_{n_2}\,\mathrm{d}\,\theta_{n_1}.\end{aligned} \tag{3.16}$$

This is the final expression for the diffuse component of the angular scattering PDF. Its evaluation involves five nested numerical integrals, which remains computationally feasible on typical modern hardware.

B. Scattering Under Locally-Specular Reflections

In the case of fully-specular local reflections, the expression of the local angular scattering kernel takes the form

$$\mathcal{K}^{ang}_{L_{spec}}\left(\theta_{i_{1_L}},\theta_{i_{2_L}}\rightarrow\theta_{l_1},\theta_{l_2}\right) = \frac{\delta(\theta_{l_1}-\theta_{i_{1_L}})}{\sin(\theta_{l_1})}\delta(\theta_{l_2}-\theta_{i_{2_L}}), \tag{3.17}$$

where $\delta:\mathbb{R}\rightarrow\mathbb{R}$, $\delta=\delta(x)$, is the Dirac delta function, being equal to 0 for $x\neq 0$ and ∞ for $x=0$. Substituting this expression into Eq. (3.8) results in

$$\begin{aligned}p^{ang}_{spec}(\theta_{r_1},\theta_{r_2}) = \frac{\sin(\theta_{r_1})}{|\mathbf{n_G}\cdot\mathbf{u_i}|}\int_0^{\frac{\pi}{2}}\int_0^{2\pi}\frac{\delta(\theta_{l_1}-\theta_{i_{1_L}})}{\sin(\theta_{l_1})}\delta(\theta_{l_2}-\theta_{i_{2_L}})\mathcal{M}(\theta_{i_1},\theta_{i_2},\theta_{n_1},\theta_{n_2})\\ \cdot p^b_{s_{2D}}\left(-\tan(\theta_{n_1})\cos(\theta_{n_2}),-\tan(\theta_{n_1})\sin(\theta_{n_2})\right)\left(1+\tan^2(\theta_{n_1})\right)^{\frac{3}{2}}\\ \cdot\left|\cos(\theta_{i_1})-\tan(\theta_{n_1})\sin(\theta_{i_1})\left(\cos(\theta_{n_2})\cos(\theta_{i_2})+\sin(\theta_{n_2})\sin(\theta_{i_2})\right)\right|\\ \cdot\sin(\theta_{n_1})\ \mathrm{d}\,\theta_{n_2}\,\mathrm{d}\,\theta_{n_1}.\end{aligned} \tag{3.18}$$

Utilising the properties of the Dirac delta function, we can eliminate the integrals in the expression of the PDF, and obtain

$$\begin{aligned}p^{ang}_{spec}(\theta_{r_1},\theta_{r_2}) = \frac{\sin(\theta_{n_1})}{\sin(\theta_{l_1})}\frac{\sin(\theta_{r_1})}{|\mathbf{n_G}\cdot\mathbf{u_i}|}\,p^b_{s_{2D}}\left(-\tan(\theta_{n_1})\cos(\theta_{n_2}),-\tan(\theta_{n_1})\sin(\theta_{n_2})\right)\left(1+\tan^2(\theta_{n_1})\right)^{\frac{3}{2}}\\ \cdot\left|\cos(\theta_{i_1})-\tan(\theta_{n_1})\sin(\theta_{i_1})\left(\cos(\theta_{n_2})\cos(\theta_{i_2})+\sin(\theta_{n_2})\sin(\theta_{i_2})\right)\right|\frac{\sin(\theta_{l_1})}{\sin(\theta_{n_1})}\Big|_{\substack{\theta_{l_1}=\theta_{i_{1_L}}\\ \theta_{l_2}=\theta_{i_{2_L}}}}.\end{aligned} \tag{3.19}$$

The task at hand now is to find the normal angles θ_{n_1} and θ_{n_2}, for which the conditions $\theta_{l_1}=\theta_{i_{1_L}}$, $\theta_{l_2}=\theta_{i_{2_L}}$ are satisfied. We know from the global and local coordinate system definitions in Section 1 that the incident and reflected unit vectors are

$$\mathbf{u_i}=\begin{bmatrix}\sin(\theta_{i_1})\cos(\theta_{i_2})\\ \sin(\theta_{i_1})\sin(\theta_{i_2})\\ -\cos(\theta_{i_1})\end{bmatrix},\qquad \mathbf{u_r}=\begin{bmatrix}\sin(\theta_{r_1})\cos(\theta_{r_2})\\ \sin(\theta_{r_1})\sin(\theta_{r_2})\\ \cos(\theta_{r_1})\end{bmatrix}. \tag{3.20}$$

Assuming specular local reflections, the corresponding local normal vector is

$$\mathbf{n_L} = \frac{\mathbf{u_r} - \mathbf{u_i}}{|\mathbf{u_r} - \mathbf{u_i}|} = \frac{1}{|\mathbf{u_r} - \mathbf{u_i}|} \begin{bmatrix} \sin(\theta_{r_1})\cos(\theta_{r_2}) - \sin(\theta_{i_1})\cos(\theta_{i_2}) \\ \sin(\theta_{r_1})\sin(\theta_{r_2}) - \sin(\theta_{i_1})\sin(\theta_{i_2}) \\ \cos(\theta_{r_1}) + \cos(\theta_{i_1}) \end{bmatrix}, \tag{3.21}$$

$$\text{with} \quad |\mathbf{u_r} - \mathbf{u_i}| = \sqrt{2\left[1 + \cos(\theta_{r_1})\cos(\theta_{i_1}) - \sin(\theta_{r_1})\sin(\theta_{i_1})\cos(\theta_{r_2} - \theta_{i_2})\right]}.$$

These relations allow the terms in Eq. (3.19) that depend on θ_{n_1} and θ_{n_2} to be written entirely in terms of the known angles θ_{i_1}, θ_{i_2}, θ_{r_1}, and θ_{r_2}. The first factor becomes

$$\begin{aligned} \left(1 + \tan^2(\theta_{n_1})\right)^2 &= \sec^2(\theta_{n_1}) = \frac{1}{\cos^4(\theta_{n_1})} \\ &= \frac{2\left(1 + \cos(\theta_{r_1})\cos(\theta_{i_1}) - 2\sin(\theta_{r_1})\sin(\theta_{i_1})\cos(\theta_{r_2} - \theta_{i_2})\right)^2}{\left(\cos(\theta_{r_1}) + \cos(\theta_{i_1})\right)^4} \\ &= |\mathbf{n_G} \cdot \mathbf{u_i}|^2 \frac{4F_k^2}{v_z^2}, \quad \text{with} \quad v_z^2 = \left(\cos(\theta_{r_1}) + \cos(\theta_{i_1})\right)^2 \end{aligned} \tag{3.22}$$

where F_k^2 and v_z^2 are the same constants defined in [4], here generalised to an out-of-plane incident direction and an inclined surface. The second factor inside the modulus, previously written as $\left|\dot{\xi}_x \sin(\theta_{i_1})\cos(\theta_{i_2}) + \dot{\xi}_y \sin(\theta_{i_1})\sin(\theta_{i_2}) + \cos(\theta_{i_1})\right|$, only requires the specular slopes $\dot{\xi}_x$ and $\dot{\xi}_y$ expressed in terms of θ_{i_1}, θ_{i_2}, θ_{r_1}, and θ_{r_2}. These are

$$\dot{\xi}_{x_{spec}} = \frac{\sin(\theta_{r_1})\cos(\theta_{r_2}) - \sin(\theta_{i_1})\cos(\theta_{i_2})}{\cos(\theta_{r_1}) + \cos(\theta_{i_1})} \quad \text{and} \quad \dot{\xi}_{y_{spec}} = \frac{\sin(\theta_{r_1})\sin(\theta_{r_2}) - \sin(\theta_{i_1})\sin(\theta_{i_2})}{\cos(\theta_{r_1}) + \cos(\theta_{i_1})}. \tag{3.23}$$

Substituting the above expressions, the scattering kernel for specular local reflections becomes

$$\begin{aligned} p_{spec}^{ang}(\theta_{r_1}, \theta_{r_2}) = \frac{4F_k^2}{v_z^2} \, p_{s2D}^{b}\left(\dot{\xi}_{x_{spec}}, \dot{\xi}_{y_{spec}}\right) \\ \cdot \left|\dot{\xi}_{x_{spec}} \sin(\theta_{i_1})\cos(\theta_{i_2}) + \dot{\xi}_{y_{spec}} \sin(\theta_{i_1})\sin(\theta_{i_2}) + \cos(\theta_{i_1})\right| \sin(\theta_{r_1}), \end{aligned} \tag{3.24}$$

which reduces to the poly-Gaussian Kirchhoff kernel derived in [4] when $\theta_{i_2} = 0°$. The slope weighting term inside the modulus plays the same role in shaping the PDF as the mixture occlusion term $\Theta(\gamma, \dot{\gamma}_x, \dot{\gamma}_y, \theta_{i_1}, \theta_{i_2})$ introduced in that study.

4. DERIVATION OF THE EROSION MODEL

In this section, we combine the statistical tools introduced earlier, namely the biased poly-Gaussian surface model from Section 2 and the scattering kernel from Section 3, to formulate a multi-scale model for the long term erosion of surfaces under AO exposure. We make three underlying assumptions in the development of this model. First, we restrict the characteristic scale of erosion induced geometric roughness to a single Gaussian autocorrelation length, R. This implies a separation of scales between the mesoscopic length at which conical morphologies emerge and the atomic length at which the underlying erosion reactions occur. Second, we assume that material removal proceeds purely along the local surface normal, neglecting any shear driven component. This is justified because AO erosion is governed primarily by surface chemistry rather than mechanical abrasion. Finally, we assume the erosion process to be locally-homogeneous, i.e. we neglect the atomic-level variations in erosion behaviour due to variations in material density and degree of crystallinity. Under these assumptions, we formulate our erosion problem in the framework of the Level-Set Method (LSM) proposed in [9]. We introduce a $\mathcal{C}^1$ continuous function

$$\Phi : \mathbb{R}^3 \times \mathbb{R} \to \mathbb{R}, \qquad (x, y, z, t) \mapsto \Phi(x, y, z, t),$$

defined in the global reference frame over the Cartesian domain

$$\Omega = \left[-\frac{L_x}{2}, \frac{L_x}{2}\right] \times \left[-\frac{L_y}{2}, \frac{L_y}{2}\right] \times \left[-\frac{L_z}{2}, \frac{L_z}{2}\right],$$

where L_x, L_y, and L_z denote the domain extents along the x, y, and z axes, respectively. At time t, the geometric surface is identified with the zero level set of Φ, namely

$$\Gamma(t) = \{(x, y, z) \in \Omega \ : \ \Phi(x, y, z, t) = 0\}. \tag{4.1}$$

Assuming $\Gamma(t)$ can be represented as a graph over the (x, y)-plane, we write

$$\Gamma(t) = \{(x, y, \xi(x, y, t)) \ : \ (x, y) \in D\}, \tag{4.2}$$

where

$$D = \left[-\frac{L_x}{2}, \frac{L_x}{2}\right] \times \left[-\frac{L_y}{2}, \frac{L_y}{2}\right]. \tag{4.3}$$

Equivalently, the height field ξ is implicitly defined by the condition

$$\Phi\big(x, y, \xi(x, y, t), t\big) = 0, \qquad (x, y) \in D. \tag{4.4}$$

We prescribe the erosion kinematics of the surface by evolving Φ according to the level-set PDE

$$\frac{\partial \Phi}{\partial t} = \mathcal{V}_E \, |\nabla \Phi| = \mathcal{V}_E \sqrt{\left(\frac{\partial \Phi}{\partial x}\right)^2 + \left(\frac{\partial \Phi}{\partial y}\right)^2 + \left(\frac{\partial \Phi}{\partial z}\right)^2}, \tag{4.5}$$

where $\mathcal{V}_E = \mathcal{V}_E(x, y, z, t)$ denotes the local erosion speed at the point (x, y, z) and time t. We decompose $\mathcal{V}_E$ into two flux-driven contributions, grouped by the number of surface interactions. Accordingly, Eq. (4.5) can be written as

$$\frac{\partial \Phi}{\partial t} = [\Delta_{FR} + \Delta_{MR}] \, |\nabla \Phi|, \tag{4.6}$$

where Δ_{FR} represents the erosion contribution from first AO-surface reflections, and Δ_{MR} collects the contributions from all multi-reflection events. We first focus on defining Δ_{FR}, since it is by far the most straightforward contribution. Consider an incident particle stream characterised by an incident velocity vector $\mathbf{v_i} = \begin{bmatrix} \sin(\theta_{i_{1_0}})\cos(\theta_{i_{2_0}}) & \sin(\theta_{i_{1_0}})\sin(\theta_{i_{2_0}}) & -\cos(\theta_{i_{1_0}}) \end{bmatrix}^T$, mass density ρ_{AO}, and molar mass μ_{AO}. The first-reflection term can then be written as

$$\Delta_{FR} = \frac{\rho_{AO}}{\rho_S} E_y\left(\theta_{i_{1_{0_L}}}, v_i, T_S\right) \frac{N_A}{\mu_{AO}} \left[\mathbf{v_i} \cdot \frac{\nabla \Phi}{|\nabla \Phi|}\right], \quad \text{with} \quad \theta_{i_{1_{0_L}}} = \arccos\left(-\mathbf{u_i} \cdot \frac{\nabla \Phi}{|\nabla \Phi|}\right) \tag{4.7}$$

where $E_y\left(\theta_{i_{1_L}}, v_i, T_S\right)$ denotes the volumetric erosion yield of the surface material (cm^3/AO), N_A is Avogadro's number, and the local surface normal is expressed in terms of the level-set functional as $\mathbf{n_L} = \nabla\Phi/|\nabla\Phi|$. Substituting Δ_{FR} into the level-set equation gives

$$\frac{\partial \Phi}{\partial t} = \frac{\rho_{AO}}{\rho_S} E_y\left(\theta_{i_{1_{0_L}}}, v_i, T_S\right) \frac{N_A}{\mu_{AO}} \left[\mathbf{v_i} \cdot \nabla \Phi\right] + \Delta_{MR} \, |\nabla \Phi|, \tag{4.8}$$

from which it is clear that the first-reflection contribution enters as a non-linear advection term, with a speed dictated by the erosion yield function $E_y\left(\theta_{i_{1_L}}, v_i, T_S\right)$. We now turn to the multi-reflection contribution Δ_{MR}, which accounts for the additional erosion driven by reflected particles that, after scattering, re-intersect the surface and produce subsequent impacts. To evaluate this term at a given surface point for secondary reflections alone, one must know the reflected particle flux emitted from every other point on the surface. Moreover, accounting for additional reflection orders leads to a combinatorial growth in the number of contributing paths, so that an explicit computation of all multi-reflection contributions becomes computationally intractable. For this reason, we instead approximate Δ_{MR} using the statistical framework developed in Section 2 and Section 3. Specifically, we approximate the statistics of the evolving surface geometry via a biased poly-Gaussian model and use this surrogate description to capture the multi-reflection contribution with sufficient accuracy. At each time t, we introduce the fitted mean and variance functions, $\mu^f, \sigma^f : \mathbb{R} \to \mathbb{R}$, $\mu^f = \mu^f(\gamma)$ and $\sigma^f = \sigma^f(\gamma)$, together with the fitted

Gaussian autocorrelation length R^f, which collectively parametrise said poly-Gaussian model. Mathematically, these quantities are fitted according to

$$\begin{aligned}\left(\mu^f, \sigma^f, R^f\right) = \underset{\mu,\sigma,R}{\arg\min} \Bigg[&\int_{-\infty}^{\infty} \left| p_h^g(\xi - \tan(\theta_s)\, x) - p_h(\xi \,|\, \mu, \sigma, R) \right|^2 \mathrm{d}\,\xi \\ &+ \int_{-\infty}^{\infty} \left| p_{s_x}^g(\dot{\xi}_x - \tan(\theta_s)) - p_{s_x}(\dot{\xi}_x \,|\, \mu, \sigma, R) \right|^2 \mathrm{d}\,\dot{\xi}_x \\ &+ \int_{-\infty}^{\infty} \left| p_{s_y}^g(\dot{\xi}_y) - p_{s_y}(\dot{\xi}_y \,|\, \mu, \sigma, R) \right|^2 \mathrm{d}\,\dot{\xi}_y \Bigg],\end{aligned} \tag{4.9}$$

where the empirical height and slope PDFs p_h^g, $p_{s_x}^g$, and $p_{s_y}^g$ are computed based on the surface geometry at time t, $\xi(x, y, t)$, as

$$p_h^g(\xi) = \frac{1}{L_x L_y} \int_{-\frac{L_x}{2}}^{\frac{L_x}{2}} \int_{-\frac{L_y}{2}}^{\frac{L_y}{2}} \delta(\xi - \xi(x, y))\, \mathrm{d}\, y\, \mathrm{d}\, x, \tag{4.10}$$

$$p_{s_x}^g(\dot{\xi}_x) = \frac{1}{L_x L_y} \int_{-\frac{L_x}{2}}^{\frac{L_x}{2}} \int_{-\frac{L_y}{2}}^{\frac{L_y}{2}} \delta\left(\dot{\xi}_x - \frac{\partial \xi(x, y)}{\partial x}\right) \mathrm{d}\, y\, \mathrm{d}\, x, \quad \text{and} \tag{4.11}$$

$$p_{s_y}^g(\dot{\xi}_y) = \frac{1}{L_x L_y} \int_{-\frac{L_x}{2}}^{\frac{L_x}{2}} \int_{-\frac{L_y}{2}}^{\frac{L_y}{2}} \delta\left(\dot{\xi}_y - \frac{\partial \xi(x, y)}{\partial y}\right) \mathrm{d}\, y\, \mathrm{d}\, x. \tag{4.12}$$

With the poly-Gaussian model fitted, we can now express the multi-reflection contribution as

$$\Delta_{MR} = \sum_{k=0}^{\infty} \left[\prod_{j=0}^{k} \vartheta_j \left(1 - \bar{\Psi}_j(\bar{\alpha}_{E_j})\right) \right] \Delta_{MR}^k(\theta_{n_1}, \theta_{n_2}, v_i, \bar{\alpha}_{E_k}), \tag{4.13}$$

where Δ_{MR}^k denotes the erosion contribution associated with particles that undergo k reflections prior to re-impact and $\bar{\alpha}_{E_k}$ is their average energy accommodation coefficient, approximated as a function of the average local energy accommodation coefficient $\bar{\alpha}_E$ by

$$\bar{\alpha}_{E_k} = 1 - (1 - \bar{\alpha}_E)^k. \tag{4.14}$$

The average local energy accommodation coefficient, $\bar{\alpha}_E$, is computed as

$$\begin{aligned}\bar{\alpha}_E = \int_0^{2\pi} \int_0^{\pi} p_{spec}^{ang} \left(\theta_{r_1}(\theta_{n_1}, \theta_{n_2}), \theta_{r_2}(\theta_{n_1}, \theta_{n_2}) \,|\, \theta_{i_{1_0}}, \theta_{i_{2_0}}\right) \\ \cdot \alpha_E \left(\theta_{i_{1_{L_0}}}, v_i, T_S\right) \sin(\theta_{n_1})\, \mathrm{d}\, \theta_{n_1}\, \mathrm{d}\, \theta_{n_2},\end{aligned} \tag{4.15}$$

where $\alpha_E \left(\theta_{i_{1_{L_0}}}, v_i, T_S\right)$ is the local energy accommodation function, dependent on the local particle incidence velocity vector and surface temperature. The factor ϑ_j is the probability that an AO particle intersects the surface again following its j^{th} reflection, while $\bar{\Psi}_j$ is the corresponding mean probability of surface reaction at that reflection order. The re-impact probability ϑ_j is given by

$$\begin{aligned}\vartheta_j = \int_0^{2\pi} \int_0^{\pi} p_{inc}^j \left(\theta_{i_{1_j}}, \theta_{i_{2_j}}\right) \int_{-\infty}^{\infty} \int_0^{2\pi} \int_0^{\pi} p_{sct}^{ang} \Big|^j \left(\theta_{r_1}, \theta_{r_2} \,|\, \theta_{i_{1_j}}, \theta_{i_{2_j}}\right) p_h(\xi_0) \\ \cdot \left[1 - \mathcal{S}^b\left(\theta_{r_1}, \theta_{r_2}, \xi_0\right)\right] \sin(\theta_{r_1})\, \mathrm{d}\, \theta_{r_1}\, \mathrm{d}\, \theta_{r_2}\, \mathrm{d}\, \xi_0\, \sin(\theta_{i_{1_j}})\, \mathrm{d}\, \theta_{i_{2_j}}\, \mathrm{d}\, \theta_{i_{2_j}},\end{aligned} \tag{4.16}$$

in which the incident-flux PDF after the j^{th} reflection, $p_{inc}^j(\theta_{i_{1_j}}, \theta_{i_{2_j}})$, is defined recursively as

$$p_{inc}^j(\theta_{i_{1_j}}, \theta_{i_{2_j}}) = \begin{cases} \displaystyle\int_0^{2\pi} \int_0^{\pi} p_{inc}^{j-1}(s_1, s_2)\; p_{sct}^{ang} \Big|^j \left(\pi - \theta_{i_{1_j}}, \theta_{i_{2_j}} \,\middle|\, s_1, s_2\right) \sin(s_1)\, \mathrm{d}\, s_1\, \mathrm{d}\, s_2, & j > 0, \\ p_{sct}^{ang} \Big|^j \left(\pi - \theta_{i_{1_j}}, \theta_{i_{2_j}} \,\middle|\, \theta_{i_{1_0}}, \theta_{i_{2_0}}\right), & j = 0. \end{cases} \tag{4.17}$$

In the same spirit, the mean reaction probability at reflection order j is written as

$$\bar{\Psi}_j = \int_0^{2\pi}\int_0^{\pi} p_{inc}^{j}\left(\theta_{i_{1_j}},\theta_{i_{2_j}}\right)\int_0^{\infty}\int_0^{2\pi}\int_0^{\pi} p_{spec}^{ang}\left(\theta_{r_1}(\theta_{n_1},\theta_{n_2}),\theta_{r_2}(\theta_{n_1},\theta_{n_2})\,|\,\theta_{i_{1_j}},\theta_{i_{2_j}}\right) \cdot p_{sct}^{vel}(v_i\,|\,\alpha_{E_j},T_S)\Psi\left(\theta_{i_{1_{L_j}}},v_i,T_S\right)\sin(\theta_{n_1})\;\mathrm{d}\,\theta_{n_1}\,\mathrm{d}\,\theta_{n_2}\,\mathrm{d}\,v_i\;\sin(\theta_{i_{1_j}})\,\mathrm{d}\,\theta_{i_{1_j}}\,\mathrm{d}\,\theta_{i_{2_j}}, \quad (4.18)$$

where $\Psi\left(\theta_{i_{1_{L_j}}},v_i,T_S\right)$ is the local reaction rate function, dependent on the local particle incidence angle and velocity, as well as the surface temperature. The local incidence angle $\theta_{i_{1_{L_j}}}$ in the same expression is written in terms of the global angles via

$$\theta_{i_{1_{L_j}}} = \arccos\Big(\sin(\theta_{i_{1_j}})\cos(\theta_{i_{2_j}})\sin(\theta_{n_1})\cos(\theta_{n_2}) + \sin(\theta_{i_{1_j}})\sin(\theta_{i_{2_j}})\sin(\theta_{n_1})\sin(\theta_{n_2}) - \cos(\theta_{i_{1_j}})\cos(\theta_{n_1})\Big). \quad (4.19)$$

Finally, the expression of the erosion contribution for particles undergoing k reflections, Δ_{MR}^{k} is given as

$$\Delta_{MR}^{k}(\theta_{n_1},\theta_{n_2},v_i,\alpha_{E_k}) = \int_0^{2\pi}\int_0^{\pi}\left[p_{inc}^{k}\left(\theta_{i_{1_k}},\theta_{i_{2_k}}\right)\right]\int_0^{\infty}\left[p_{sct}^{vel}(v_r\,|\,\alpha_{E_k},T_S)\right] \quad (4.20)$$

$$\cdot\int_{-\infty}^{\infty}\int_0^{2\pi}\int_0^{\frac{\pi}{2}}\left[p_{sct}^{ang}\left(\pi-\theta_{r_1}(\theta_{l_1},\theta_{l_2}),\,\theta_{r_2}(\theta_{l_1},\theta_{l_2})+\pi\,\middle|\,\theta_{i_{1_j}},\theta_{i_{2_j}}\right)\right] \cdot\left[p_h(\xi_0)\right]\left[1-\mathcal{S}\left(\theta_{r_1}(\theta_{l_1},\theta_{l_2}),\,\theta_{r_2}(\theta_{l_1},\theta_{l_2}),\,\xi_0\right)\right]\left[E_y\left(\theta_{l_1},v_r,T_S\right)\right] \quad (4.21)$$

$$\cdot\left[v_i\frac{\rho_{AO}}{\rho_S}\frac{N_A}{\mu_{AO}}\right]\left[\cos(\theta_{l_1})\sin(\theta_{l_1})\right]\;\mathrm{d}\,\theta_{l_1}\;\mathrm{d}\,\theta_{l_2}\;\mathrm{d}\,\xi_0\;\mathrm{d}\,v_r\;\mathrm{d}\,\theta_{i_{1_k}}\;\mathrm{d}\,\theta_{i_{2_k}},$$

where the incident-angle PDF $p_{inc}^{k}\left(\theta_{i_{1_k}},\theta_{i_{2_k}}\right)$ is evaluated recursively according to Eq. (4.17). The resulting erosion kinematics are therefore governed by

$$\frac{\partial\Phi}{\partial t} = \frac{\rho_{AO}}{\rho_S}E_y\left(\theta_{i_{1_L}},v_i,T_S\right)\frac{N_A}{\mu_{AO}}\left[\mathbf{v_i}\cdot\nabla\Phi\right] + \sum_{k=0}^{\infty}\left[\prod_{j=0}^{k}\vartheta_j\left(1-\bar{\Psi}_j(\alpha_{E_j})\right)\right]\Delta_{MR}^{k}(\theta_{n_1},\theta_{n_2},v_i,\alpha_{E_k})\,|\nabla\Phi|\,. \quad (4.22)$$

This evolution equation is posed on the computational domain and closed by periodic boundary conditions on the planes $x = \pm L_x/2$ and $y = \pm L_y/2$. On the planes $z = \pm L_z/2$ we impose homogeneous Neumann conditions, i.e. $\partial\Phi/\partial z = 0$. The level-set functional is initialised at $t = 0$ as

$$\Phi(x,y,z,0) = \begin{cases} 1 & z > \xi(x,y,t=0); \\ -1 & z \le \xi(x,y,t=0). \end{cases} \quad (4.23)$$

To solve the problem, it suffices to prescribe the material-specific erosion yield and reaction probability, $E_y(\theta_{i_{1_L}},v_i,T_S)$, $\Psi(\theta_{i_{1_L}},v_i,T_S)$ and $\alpha_E(\theta_{i_{1_L}},v_i,T_S)$. In this work, all three functions are obtained from reactive molecular dynamics simulations performed with the Large-scale Atomic/Molecular Massively Parallel Simulator (LAMMPS) package [10] and the ReaxFF [11] reactive force field.

REFERENCES

[1] P. Beckmann. "Shadowing of random rough surfaces". In: *IEEE Transactions on Antennas and Propagation* 13.3 (May 1965), pp. 384–388. ISSN: 0096-1973. DOI: 10.1109/tap.1965.1138443.

[2] P. Beckmann. "Scattering by non-Gaussian surfaces". In: *IEEE Transactions on Antennas and Propagation* 21.2 (1973), pp. 169–175. DOI: 10.1109/TAP.1973.1140444.

[3] Peter Beckman, Andre Spizzichino, and Petr Beckmann. *The scattering of electromagnetic waves from rough surfaces*. Radar Library. Norwood, MA: Artech House, Mar. 1987.

[4] Sabin-Viorel Anton et al. "A Wave Scattering Approach to Modelling Surface Roughness in Orbital Aerodynamics". In: *Advances in Space Research* (May 2025). ISSN: 0273-1177. DOI: 10.1016/j.asr.2025.05.069. URL: http://dx.doi.org/10.1016/j.asr.2025.05.069.

[5] M. Ya. Litvak and V. I. Malyugin. "Poly-Gaussian models of a non-Gaussian randomly rough surface". In: *Technical Physics* 57.4 (Apr. 2012), pp. 524–533. ISSN: 1090-6525. DOI: 10.1134/s1063784212040172.

[6] Kim K. de Groh and Bruce A. Banks. *Atomic oxygen erosion data from the MISSE 2-8 missions - NASA technical reports server (NTRS)*. 2019. URL: https://ntrs.nasa.gov/citations/20190025445.

[7] Bruce A. Banks et al. *Comparison of atomic oxygen erosion yields of materials at various energy and impact angles - NASA technical reports server (NTRS)*. 2006. URL: https://ntrs.nasa.gov/citations/20060047719.

[8] B. Smith. "Geometrical shadowing of a random rough surface". In: *IEEE Transactions on Antennas and Propagation* 15.5 (1967), pp. 668–671. DOI: 10.1109/TAP.1967.1138991.

[9] Stanley Osher and James A Sethian. "Fronts propagating with curvature-dependent speed: Algorithms based on Hamilton-Jacobi formulations". In: *Journal of Computational Physics* 79.1 (Nov. 1988), pp. 12–49. ISSN: 0021-9991. DOI: 10.1016/0021-9991(88)90002-2. URL: http://dx.doi.org/10.1016/0021-9991(88)90002-2.

[10] A. P. Thompson et al. "LAMMPS - a flexible simulation tool for particle-based materials modeling at the atomic, meso, and continuum scales". In: *Comp. Phys. Comm.* 271 (2022), p. 108171. DOI: 10.1016/j.cpc.2021.108171.

[11] Adri C. T. van Duin et al. "ReaxFF: A Reactive Force Field for Hydrocarbons". In: *The Journal of Physical Chemistry A* 105.41 (Sept. 2001), pp. 9396–9409. ISSN: 1520-5215. DOI: 10.1021/jp004368u. URL: http://dx.doi.org/10.1021/jp004368u.